Chemical Physics Letters 463 (2008) 160–165

Contents lists available at ScienceDirect

Chemical Physics Letters

journal homepage: www.elsevier.com/locate/cplett

Ultrafast energy transfer from 3-mercaptopropionic acid-capped CdSe/ZnS QDs to dye-labelled DNA

S. Shankara Narayanan, Sudarson Sekhar Sinha, Pramod Kumar Verma, Samir Kumar Pal *

Unit for Nano Science and Technology, Department of Chemical, Biological and Macromolecular Sciences, S. N. Bose National Centre for Basic Sciences, Block JD, Sector III, Salt Lake, Kolkata 700 098, India

ARTICLE INFO

Article history:
Received 6 June 2008
In final form 13 August 2008
Available online 17 August 2008

ABSTRACT

Femtosecond-resolved fluorescence upconversion and picosecond-resolved spectroscopic measurements have been employed to confirm a highly efficient ultrafast FRET from MPA-capped CdSe/ZnS QDs to dye molecules attached to dodecamer DNA. It appears that hydrogen bonding is the associative mechanism between the MPA-capped QDs and DNA. High FRET efficiency of 92% together with the estimated donor–acceptor distance suggests that the adsorptive interactions between DNA and MPA-capped QDs result in a conformation in which DNA lies along the surface of the QD. Circular dichroism studies have been performed which reveal some perturbation in the native B-form of DNA in the nanobioconjugate.

1. Introduction

Over the past decades, quantum dots (QDs) have been studied in detail owing to their unique size-dependent optical and electrical properties [1,2]. Particularly, interest in the unique optical properties of QDs has resulted in the development of QD-bioconjugates for imaging [3–6] and diagnostics [7–10]. In this regard, many groups have reported the attachment of biological molecules to water-soluble nanocrystals [11,12] through different types of interactions. In the most primitive case the molecules are simply adsorbed either directly to the nanoparticle surface or to the shell of stabilizing molecules around the nanoparticles [13,14]. Other approaches have used the covalent conjugation method via the formation of chemical bonds between the biological molecules and the stabilizing shell around the nanoparticles [12,15,16]. In addition to these, formation of nanobioconjugates through various nonspecific interactions (electrostatic, hydrogen-bonding interactions etc.) between biological molecules and nanoparticles have been explored by several groups [17–19]. A myriad of nanobioconjugates using proteins [10,20] and oligonucleotides [9,15,21,22] have already been successfully employed for various applications such as sensors for the detection of molecules [7,23,24] or the labeling of cells [16,25,26].

Core–shell CdSe/ZnS QDs are probably the most successful type of QDs that have been developed and remained the best available for biological applications [12,26]. Out of a variety of techniques developed, heterobifunctional ligands such as thiol-alkyl acids have been one of the most commonly used surface chemistry for the water solubility and bioconjugation of CdSe/ZnS QDs. Commonly used thiol-alkyl acids include mercaptoacetic acid [12,27] (MAA), 3-mercaptopropionic acid [15,21,22,28] (MPA), and dihydrolipoic acid [7,8,10]. The major advantage of using thiol-alkyl acid surface chemistry lies in the fact that these short-chain mercapto-carbonic ligands provide a very compact water solubilizing shell around the CdSe/ZnS QDs. Hence, these QDs are highly suited for Förster resonance energy transfer (FRET)-based studies and applications. There are many reports in the literature on the FRET between CdSe/ZnS QD and biomolecule/dye-labelled biomolecule [8,10,21,29]. For example, Zhou et al. [21] have reported an efficient FRET between CdSe/ZnS QD and dye-labeled DNA in both bulk solution and at the single molecule level. FRET has been demonstrated between CdSe/ZnS QDs and green fluorescent proteins employing both steady-state and time-resolved spectroscopic techniques [29]. Using femtosecond transient absorption spectroscopy, Neuman et al. [30] have reported FRET between water-soluble CdSe/ZnS QDs and several transition metal complexes. Ultrafast energy transfer from photoexcited single CdSe/ZnS QDs to Ag nanoparticles has also been demonstrated [31]. In another recent report, adsorptive interactions between oligonucleotides and MAA-capped QDs using the sensitivity of FRET to the proximity between a QD donor and Cy3 acceptor were explored and the results obtained were rationalized in terms of an electrostatic and hydrogen-bonding model [19]. The same group also demonstrated the use of MAA-capped QDs in a FRET-based approach to two-color nucleic acid diagnostics [32].

In the present work, using femtosecond-resolved fluorescence upconversion and picosecond-resolved photoluminescence measurements, we report an efficient ultrafast energy transfer from 3-mercaptopropionic acid-capped CdSe/ZnS QDs (donor) to Ethidium bromide-labeled-DNA (acceptor) using the sensitivity of FRET. Furthermore, in order to confirm any structural perturbation

* Corresponding author. Fax: +91 33 2335 3477.
E-mail address: skpal@bose.res.in (S.K. Pal).

0009-2614/$ - see front matter © 2008 Elsevier B.V. All rights reserved.
doi:10.1016/j.cplett.2008.08.057

of DNA in the nanobioconjugate, circular dichroism (CD) studies have been performed on both DNA and DNA-QD conjugate.

2. Materials and methods

Adirondack Green CdSe/ZnS core/shell semiconductor nanocrystals (QDs) in toluene were from Evident Technologies (Troy, NY) and had an emission maximum of 522 nm and a core diameter of 2.1 nm. Chloroform (Sigma), 3-mercaptopropionic acid, MPA (99%, SRL, Mumbai) and tertramethylammonium hydroxide (Spectrochem., Mumbai) were used as received without further purification. Phosphate buffer was obtained from Sigma. The probe Ethidium bromide (EB) was obtained from Molecular Probes. The DNA oligomer having sequence CGCGAATTCGCG was obtained from Sigma–Aldrich, purified by HPLC technique, and checked by gel electrophoresis. The gel electrophoresis result indicated a single spot consistent with pure dodecamer DNA. All the aqueous solutions were prepared in 10 mM phosphate buffer pH 7 using water from the Millipore system. To reassociate the single strand DNA into self-complimentary double-strand DNA $(CGCGAATTCGCG)_2$, thermal annealing was performed as per the methodology prescribed by the vendor. The oligomer was dialyzed exhaustively against phosphate buffer prior to further use. The nucleotide concentrations were determined by absorption spectroscopy using the average extinction coefficient per nucleotide of the DNA ($6600\ M^{-1}\ cm^{-1}$ at 260 nm). The EB-DNA complex solution was prepared by adding the requisite amount of probe stock solution to DNA followed by 1 h stirring. To ensure complete complexation of EB with the DNA, the probe concentration was made much less (2.5 μM) than that of the DNA (10 μM) ([EB-DNA] = 2.5 μM) for the FRET studies.

The TOPO-capped CdSe/ZnS QDs in toluene were rendered water-soluble by ligand exchange with MPA following a recent literature procedure [33] where the reactivity of the thiol group with the ZnS surface was enhanced by the formation of thiolate anion using an organic base. The final colloidal solution of MPA-capped CdSe/ZnS QDs was exhaustively dialyzed against phosphate buffer (10 mM, pH 7.0) using a dialysis membrane (Spectrum Laboratories, Inc, USA) with a molecular weight cut-off at 12 000–14 000 Da. The concentration of the resulting MPA-QDs was determined by absorption spectroscopy using the first absorption peak at 505 nm. The quantum yield (QY) of TOPO-capped QDs i.e. QDs before MPA capping was 0.4. The QY of the MPA-capped QD was determined using the TOPO-capped QDs as the reference (QY = 0.4) and found to be 0.16. Adsorption of DNA onto the surface of MPA-modified CdSe/ZnS QDs was done by mixing QD ([QD] = 0.2 μM) and EB-labeled DNA aqueous samples, having a final [QD]:[EB-DNA] = 1:12.5, for at least 1 h and used for FRET studies.

Steady-state absorption and emission were measured with Shimadzu Model UV-2450 spectrophotometer and Jobin Yvon Model Fluoromax-3 fluorimeter, respectively. Circular dichroism (CD) experiments were done in a JASCO 815 spectropolarimeter. The femtosecond-resolved fluorescence spectroscopy was measured using a femtosecond upconversion setup (FOG 100, CDP) in which the sample was excited at 365 nm, using the second harmonic of a mode-locked Ti-sapphire laser with an 80 MHz repetition rate (Tsunami, Spectra Physics), pumped by 10 W Millennia (Spectra Physics). The fundamental beam of 730 nm was frequency doubled in a nonlinear crystal (1 mm BBO, $\theta = 5°$, $\phi = 90°$). The fluorescence (at 528 nm) emitted from the sample is mixed with the fundamental beam (730 nm) to yield an upconverted photon signal of 306.4 nm in a nonlinear crystal (0.5 mm BBO, $\theta = 10°$, $\phi = 90°$). The upconverted light was dispersed in a double monochromator and detected using photon counting electronics. A cross-correlation function obtained using the Raman scattering from water displayed a full width at half maximum (FWHM) of 165 fs. The femtosecond fluorescence decays were fitted using a Gaussian shape for the exciting pulse.

Picosecond-resolved fluorescence transients were measured and fitted by using commercially available spectrophotometer (LifeSpec-ps) from Edinburgh Instruments, UK (excitation wavelength 375 nm, 80 ps instrument response function, (IRF)). The observed fluorescence transients were fitted by using a nonlinear least square fitting procedure to a function $(X(t) = \int_0^t E(t')\,R(t-t')\mathrm{d}t')$ comprising of convolution of the IRF ($E(t)$) with a sum of exponentials $(R(t) = A + \sum_{i=1}^{N} B_i e^{-t/\tau_i})$ with pre-exponential factors (B_i), characteristic lifetimes (τ_i) and a background (A). Relative concentration in a multiexponential decay was finally expressed as; $c_n = \frac{B_n}{\sum_{i=1}^{N} B_i} \times 100$. The quality of the curve fitting was evaluated by reduced chi-square and residual data.

To estimate the FRET efficiency of the donor and hence to determine the distance of the donor–acceptor pair, we followed the methodology described in chapter 13 of Ref. [34]. The Förster distance (R_0) is given by

$$R_0 = 0.211[\kappa^2 n^{-4} Q_D J(\lambda)]^{1/6} \quad (\text{in Å}) \tag{1}$$

where κ^2 is a factor describing the relative orientation in space of the transition dipoles of the donor and acceptor. For donor and acceptors that randomize by rotational diffusion prior to energy transfer, the magnitude of κ^2 is assumed to be 2/3. In the present study the same assumption has been made. The refractive index (n) of the medium was assumed to be 1.4. Q_D, the quantum yield of the donor QD in the absence of acceptor, was 0.16. $J(\lambda)$, the overlap integral, which expresses the degree of spectral overlap between the donor emission and the acceptor absorption. Once the value of R_0 is known, the donor–acceptor distance (R) can easily be calculated using the formula

$$R^6 = [R_0^6(1 - E)]/E \tag{2}$$

Here E is FRET efficiency, measured by using the lifetimes of the donor in the absence (τ_D) and presence (τ_{DA}) of acceptor.

$$E = 1 - (\tau_{DA}/\tau_D). \tag{3}$$

It has to be noted that Eq. (3) holds rigorously only for a homogeneous system (i.e. identical donor–acceptor complexes) in which the donor and the donor–acceptor complex have single exponential decays. However, for donor–acceptor systems decaying with multiexponential lifetimes [34], FRET efficiency (E) is calculated from the amplitude weighted lifetimes $\langle\tau\rangle = \sum_i \alpha_i \tau_i$ where α_i is the relative amplitude contribution to the lifetime τ_i. We have used the amplitude weighted time constants for τ_D and τ_{DA} to evaluate E using Eq. (3).

3. Results and discussion

Inset of Fig. 1a illustrates the absorption and emission spectra of MPA-capped CdSe/ZnS QDs in buffer which remained largely unchanged after the ligand-exchange procedure. HRTEM image (inset of Fig. 1b) of QDs reveals an average diameter of 4–4.5 nm with a honeycomb structure. The existence of lattice fringes illustrates the highly crystalline nature of the QDs. There was however, a slight red shift of ~6 nm in the peak of the emission band of aqueous sample as compared to toluene sample (522 nm). Furthermore, when the fluorescence intensity at 528 nm was measured as a function of the excitation wavelength (280–450 nm), both the toluene and aqueous samples yielded similar emission profiles and intensities. Taken all together, it indicates that the QDs retained their photoluminescence properties when transferred into water using the literature procedure, which is important for fully

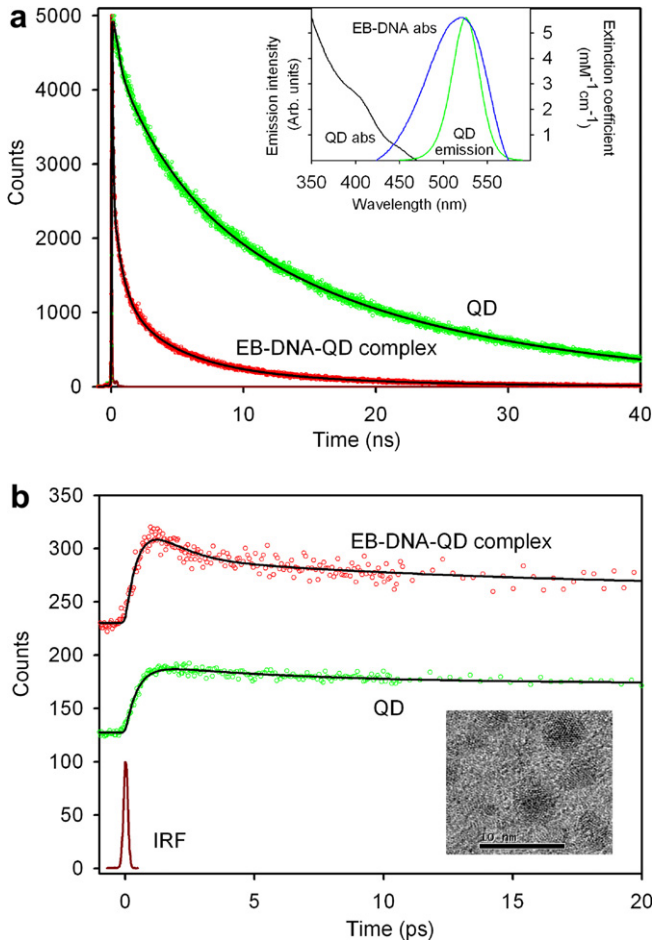

Fig. 1. (a) Picosecond-resolved PL transients (instrument response function, IRF = 80 ps) of MPA-capped CdSe/ZnS QDs and (EB-DNA)-QD complex monitored at λ_{em} = 528 nm. Inset shows the steady-state absorption spectrum of MPA-capped CdSe/ZnS core–shell QDs in buffer together with the spectral overlap between emission spectrum of QDs and the absorption spectrum of EB-labeled DNA (the extinction coefficient value is for the acceptor, EB-labelled DNA). (b) Femtosecond-resolved fluorescence upconversion decay of MPA-capped CdSe/ZnS core–shell QDs and QD-(EB-DNA) complex monitored at λ_{em} = 528 nm. The dark red decay is the IRF (instrument response function) of the femtosecond pulse. Inset shows the HRTEM image of QD.

harnessing the superior qualities of these fluorescent nanocrystals for applications in aqueous media. The MPA-capped QDs were very stable and remained clear in the solution even after keeping it in room temperature for 1 month with no signs of precipitation. It has been previously confirmed from the XPS studies [33] that the coverage of the MPA on the QDs was about 85%. The direct bonding of MPA ligands onto the QD surface ensured that the overall size of the QDs remained small with a thin solubilizing shell to increase the efficiency for energy transfer, which is important for FRET applications.

In order to achieve high conjugation (FRET) efficiency between the QD and the EB-labeled DNA, it was found necessary to remove the excessive unbound MPA used to make the QD water-soluble. This was achieved by exhaustive dialysis of the MPA-QD sample against the phosphate buffer (pH 7.0). Removal of the excess MPA eliminates the competition for QD binding from MPA, and is known to increase the FRET efficiency of the QD to EB-DNA [21]. The pH of the final solution of MPA-capped CdSe/ZnS QDs was 7.0. In a recent study on the adsorptive interactions between MAA-capped CdSe/ZnS QDs and oligonucleotides [19], it has been reported that at neutral pH, there is likely a mixture of protonated and deprotonated carboxyl groups of MAA. The study also revealed that the adsorption of DNA onto the surface of QDs was roughly 3–4 folds stronger than that in borate buffer at pH 9.5 which was rationalized in terms of an electrostatic and hydrogen-bonding model. The same mechanism of hydrogen-bonding interactions between oligonucleotides (involving nucleobases) and MPA-capped CdSe/ZnS QDs are expected to play the dominant role in the adsorption of DNA onto the surface of MPA-capped QDs. However, it should be noted that changes in the protonation state of MPA with pH also induce changes in the surface charge which can drastically change the adsorption of QDs to DNA [19].

The inset of Fig. 1a reveals a huge spectral overlap between the emission spectrum of QDs and the absorption spectrum of EB-DNA complex suggesting that efficient FRET between the donor (QDs) and the acceptor (EB-labeled DNA) can take place when DNA is adsorbed onto the surface of QDs. We confirmed that only a slight overlap between the donor and acceptor fluorescence occurred, allowing for the effective separation of donor fluorescence from that of the acceptor. Hence, we expect that the adsorption of EB-labeled-DNA onto the surface of MPA-capped QDs will result in the quenching of the QD fluorescence at 528 nm, while at the same time enhancing the EB fluorescence at 600 nm through FRET which was confirmed through both steady-state and time-resolved experiments as described below. Fig. 1a shows the picosecond-resolved PL transients of QD and QD-(EB-DNA) conjugate at 528 nm. The picosecond decay of QDs in buffer revealed multiexponential [35] time constants of 0.31 ns (28%), 4.83 ns (26%) and 19.44 ns (46%) giving an average time constant ($\langle\tau\rangle$) of 10.3 ns. For the donor–acceptor system i.e. QD-(EB-DNA) complex, the time constants obtained were 64 ps (73%), 0.7 ns (14%), 3.85 ns (9%) and 11.54 ns (4%) revealing an average time constant ($\langle\tau\rangle$) of 0.92 ns. The substantial shortening in the QD exciton lifetime upon conjugate formation indicate conclusively that efficient FRET occurs from the QD donor to the EB-DNA acceptor. Based on the spectral overlap and using Eq. (3), we estimated a FRET efficiency of 92% in our FRET system. The Förster distance, R_0, for the QD-(EB-DNA) complex measured using Eq. (1) is 3.2 nm. Estimation of FRET efficiency from steady-state experiment has been provided in Supplementary material. In order to obtain the ultrafast component in the FRET system which was missing in our picosecond measurements due to its limited IRF, we performed femtosecond fluorescence upconversion measurements.

For CdSe/ZnS QDs (donor) in buffer, the upconverted fluorescence decay (Fig. 1b) revealed an ultrafast rise component of 430 fs together with a shorter decay component of 6 ps. The ultrafast rise time of 430 fs is attributed to the buildup of the lowest (1S) electron state in CdSe/ZnS QDs and is consistent with the femtosecond transient absorption measurements on colloidal CdSe QDs having a radius of 4.2 nm by Klimov and McBranch [36] where they reported a rise time of ~400 fs. Using femtosecond fluorescence upconversion technique, Underwood et al. [37] reported a rise time of ~530 fs for the 72 Å CdSe QDs compared to ~270 fs for the 30 Å CdSe QDs. Energy relaxation following the optical excitation leads to the establishment of quasi-equilibrium populations of electron and hole quantized states. Depopulation of these states can occur via a variety of radiative and non-radiative mechanisms. The most important processes competing with the radiative ones are carrier trapping at surface/interface states. The short-lived component, representing the lifetime of fluorescence decay at the band edge, comprises both a radiative decay from electron–hole recombination and a non-radiative decay via trap states [38]. Because of the surface passivation of the core CdSe QDs with ZnS shell, the surface trapping process can be assumed to be negligible. Hence, the fast relaxation time constant of 6 ps could be assigned to the direct recombination of the exciton [39]. However, the contribution of surface states in the decay component of 6 ps cannot be completely ruled out due to the presence of MPA at the outer

surface of QDs which has the ability to act as hole traps for these QDs [40]. We also obtained a slow decay component of 310 ps in the femtosecond measurement which was also confirmed in the picosecond-resolved experiment. Together with 310 ps, picosecond-resolved decays of QDs (Fig. 1a) in buffer also revealed time constants of 4.8 ns and 19.4 ns. The picosecond-resolved decay time constants of donor and donor–acceptor systems together with their average time-constants ($\langle\tau\rangle$) have been listed in Table 1. The long-lived component of ~10 ns could be assigned to the radiative recombination of the carriers bound to trap states [41] or due to the relaxation from a triplet state to the ground state [37]. We have also measured the femtosecond dynamics of QD-(EB-DNA) complex (donor–acceptor system) and obtained a rise component of 640 fs, decay components of 935 fs and 13 ps, and a long component of 269 ps in the fitted decay (Fig. 1b). The faster decay time scales for the donor–acceptor system compared to donor alone conclusively indicates an efficient ultrafast energy transfer from the MPA-capped CdSe/ZnS QDs to the adsorbed EB-DNA complex. The femtosecond-resolved decay time constants of donor and donor–acceptor systems together with their average time-constants ($\langle\tau\rangle$) have been listed in Table 1. The FRET efficiency obtained from the femtosecond experiment was found to be 91% similar to that obtained from picosecond measurements. It has to be mentioned that the percentage of donor QDs which contribute to FRET, specified by the percentage of the additional faster component in the time-resolved fluorescence decay of QD-(EB-DNA) complex (at 528 nm), which is absent in the donor fluorescence, has been estimated to be ~75%. Hence, assuming 1:1 complexation (see below) of QD (0.2 μM initial concentration) with EB-DNA, it implies that 0.15 μM of QD will be complexed with the same amount of EB-DNA. Since the total concentration of DNA used was 10 μM, it implies a significant percentage of DNA do not take part in FRET.

In order to determine the binding constant and to get an estimate for the number of duplex DNAs bound per QD, we have performed luminescence titration experiments of QDs with EB-DNA complex. Fractional changes in luminescence of QDs as a function of EB-DNA concentration were fitted to the Frisch–Simha–Eirich (FES) adsorption isotherm [42] to extract binding constant

$$[\theta \exp(2K_1\theta)]/(1-\theta) = (KC)^{1/\nu} \quad (4)$$

where θ, the fractional surface coverage, is equated to fractional change in luminescence [43]; C is the EB-DNA concentration; K_1 is a constant that is a function of the interaction of adsorbed polymer segments and is set equal to 0.5 [44]; K is the equilibrium constant for binding of EB-DNA ([EB]:[DNA] = 1) to MPA-capped CdSe/ZnS QDs; and ν is the average number of segments attached to the surface. Our definition of θ implicitly assumes a two-state model for the nanoparticle-DNA interaction [14]; the nanoparticle is either bound to an EB-DNA or free of EB-DNA. In a typical titration experiment, 1 mL of QD (1 μM) was taken and its emission spectrum was recorded. Different aliquots of a 300 μM EB-DNA ([EB]:[DNA] = 1) were then added to the nanoparticle solution (1 μM) and emission spectra were recorded after 20 min of equilibration time per aliquot. The inset of Fig. 2 reveals the emission quenching of the nanoparticle solution at 528 nm on addition of EB-DNA and a corresponding increase in the EB-DNA emission intensity at

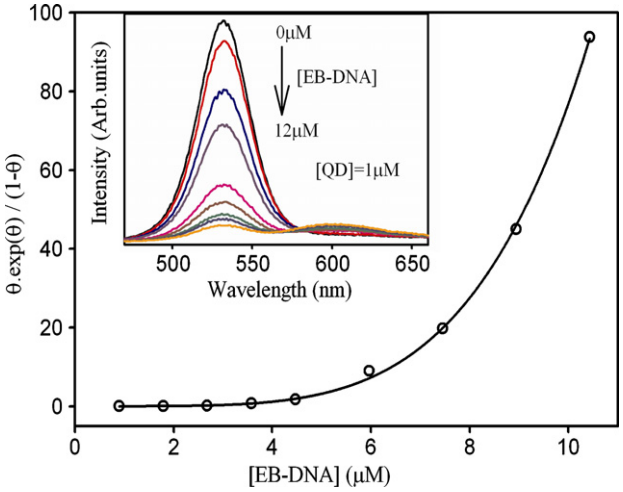

Fig. 2. Frisch–Simha–Eirich plot for EB-DNA adsorption to CdSe/ZnS QDs. The best fit was obtained for $K_1 = 0.5$ and $\nu = 0.298$. Inset shows the photoluminescence spectra of MPA-capped CdSe/ZnS QDs (1 μM) upon addition of (from the top) 0, 1.8, 2.7, 3.6, 4.5, 6, 7.5, 9, 10.5 and 12 μM EB-DNA solution.

600 nm due to FRET from QD to EB-DNA. Fig. 2 clearly reveals that our data fits best with the model, with $K \sim 2.5 \times 10^5\ M^{-1}$.

By monitoring the relative percentage of the bound QDs which are undergoing energy transfer with EB-DNA complex from the picosecond-resolved fluorescence transients of the QD-(EB-DNA) complex ([EB]:[DNA] = 1), the binding constant (K) of the EB-DNA complex with the QDs was calculated using following equation:

$$K = \left[\frac{[QD-(EB-DNA)]}{([QD]-[QD-(EB-DNA)]) \times ([EB-DNA]-[QD-(EB-DNA)])}\right] \quad (5)$$

The binding constant, K obtained for the final aliquot of EB-DNA added to QD i.e. [QD:EB-DNA] = 1:12, using Eq. (5) is $2.0 \times 10^5\ M^{-1}$, which is close to the value of binding constant obtained from FES plot (Fig. 2). Hence the above equation support FES model very well (which assumes all DNA is either free or bound to a QD) and confirms that, on average, one DNA adsorbs onto the surface of one QD. We obtained similar time constants for each aliquot of DNA added to QD suggesting that only the percentage of QD complexed to EB-DNA changes whereas the FRET efficiency remains the same. Moreover, the binding constant calculated for each aliquot of EB-DNA added to QDs in the titration experiment gave a similar value of $(2.0 \pm 0.2) \times 10^5\ M^{-1}$. These observations clearly indicate that the QD and EB-DNA form a 1:1 complex for all concentrations of EB-DNA, particularly in the concentration used in our experiments. To confirm that the fluorescence quenching observed here is due to FRET only, a titration experiment with free DNA only (without intercalated EB) has been performed. We found negligible quenching of the QD emission with each aliquot of DNA added. Moreover, time-resolved decays of QD and QD-DNA were found to be almost overlapping each other. These studies clearly points out that the mechanism behind the quenching of QDs is only FRET.

Table 1
Fitted decay time constants of QD and QD-(EB-DNA) complex from picosecond and femtosecond experiments

System	Picosecond experiment					Femtosecond experiment			
	τ_1 (α_1) (ns)	τ_2 (α_2) (ns)	τ_3 (α_3) (ns)	τ_4 (α_4) (ns)	$\langle\tau\rangle$ (ns)	τ_1 (α_1) (ps)	τ_2 (α_2) (ps)	τ_3 (α_3) (ps)	$\langle\tau\rangle$ (ps)
QD	0.31 (0.28)	4.83 (0.26)	19.44 (0.46)	–	10.3	5.9 (0.27)	634.2 (0.73)	–	466.4
QD-EB-DNA	0.064 (0.73)	0.7 (0.14)	3.85 (0.09)	11.54 (0.04)	0.92	0.93 (0.77)	13.3 (0.1)	269 (0.13)	36.4

It is known that the diameter of the CdSe core is 2.1 nm and the thickness of shell is approximately 1 nm (Evident Technologies). Also, the size of the MPA molecule is approximately 0.6 nm. Taken together, the radius of the MPA-capped CdSe/ZnS QD will be 2.6 nm. The estimated QD radius is in good agreement with the donor–acceptor distance of ~2.5 nm from the center of the QD core to the surface of the QD where (EB-DNA) will bind, suggesting that DNA molecules are adsorbed onto the surface of QDs through the hydrogen-bonding interactions. Due to the small length of the DNA (12-merDNA) and hence its high flexibility, it is expected that the DNA molecules can adopt a conformation that lies along the surface of the MPA-capped QD analogous to the observation made for the adsorption of mixed base oligonucleotides on MAA-capped CdSe/ZnS QDs [19]. It has to be mentioned that the most probable location for the intercalation of EB to dodecamer DNA is between the central AT base pair. However, EB-intercalation on the GC sites can not be completely ruled out. Nevertheless, the difference in the distances in the two locations of EB in the dodecamer is expected to be negligibly small, considering the fact that the dodecamer interact length-wise with the QDs.

In order to confirm any structural perturbation in the native structure of the DNA after the adsorption of DNA onto the surface of QDs, we carried out circular dichroism (CD) studies. As shown in Fig. 3, the CD spectrum of the hybridized DNA reveals that the DNA used in our studies were in a B-form, as evidenced by a negative band at 248 nm and a positive band at 280 nm [45,46]. In the QD-DNA conjugated system, the CD spectrum (Fig. 3) shows some broadening of the negative band at 248 nm, a slight red shift of the positive band at 280 nm and a considerable absorption in the longer wavelength (>300 nm) indicating some perturbation of the DNA structure. The broadening of the negative band of DNA at 248 nm has also been observed by Jin et al. [47] for the DNA-linked gold nanoparticle assemblies and attributed to the interconnection of the duplex DNA within the nanoparticle aggregate. Our group also recently reported such a change in the DNA conformation on encapsulation inside a reverse micelle and the result was interpreted as a characteristic of the B → Ψ-form transition [46]. The transition was associated with the condensation of the DNA in the nanospace. Our observation of the CD spectrum of the dodecamer with the QD is consistent with the condensed form of the DNA at the QD surface. The condensed form is possible for the short length DNA (dodecamer DNA) used in our experiment since it could easily wrap around the QD due to its more flexibility resulting in a highly efficient FRET (92%) between QDs and EB. Such perturbation in the DNA structure could hinder their applications as labels in immunoassays, cellular-labeling and for in vivo and deep-tissue imaging. However, this perturbation in the DNA, caused by QD-induced DNA bending, could be correlated with regulatory functions of proteins including damage recognition [48]. Recent computer simulations suggest that large structural changes in DNA can occur upon substrate (protein) binding that are solely due to changes in the solvent and ionic environment around DNA, suggesting an induced fit process [49].

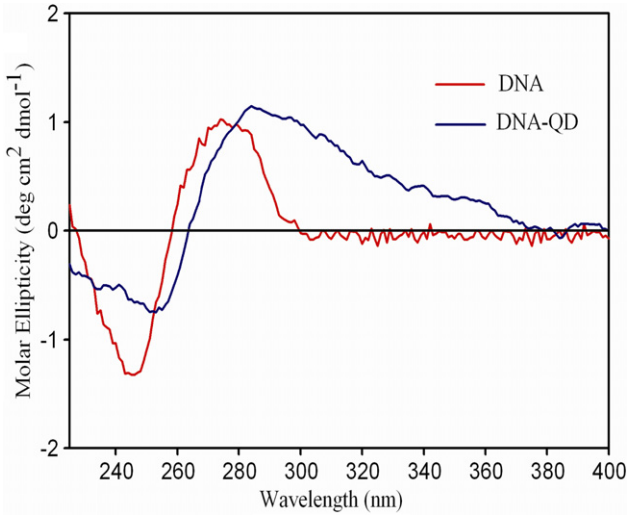

Fig. 3. Circular dichroism (CD) spectra of DNA and DNA-QD conjugate. Structural perturbation of the DNA in the conjugate is clearly evident.

4. Conclusion

Using femtosecond-resolved fluorescence upconversion and picosecond-resolved spectroscopic measurements, we have demonstrated a highly efficient ultrafast FRET from MPA-capped CdSe/ZnS QDs to EB-DNA. It appears that the hydrogen-bonding interaction between the nucleobases of DNA and the protonated carboxyl surface groups of the QDs is the mechanism behind the association of QDs to DNA. Because of a huge spectral overlap between the emission spectrum of QDs and absorption spectrum of EB-labeled DNA, a highly FRET efficiency of 92% has been obtained in our studies. The high FRET efficiency and the corresponding donor–acceptor distance of 2.5 nm suggest that adsorptive interactions between the DNA molecules and MPA-capped QDs result in a conformation that lies across the surface of the QD. CD studies on the QD-DNA conjugate indicate some perturbation in the native B-form of DNA which is probably due to the condensed form of conformation adopted by DNA. It is anticipated that this study may prove to be useful in making sensitive FRET-based sensors.

Acknowledgements

S.S.N. and P.K.V. thank CSIR, India for fellowship. We thank DST for financial Grant (SR/FTP/PS-05/2004).

Appendix A. Supplementary material

Supplementary data associated with this article can be found, in the online version, at doi:10.1016/j.cplett.2008.08.057.

References

[1] A. Henglein, Chem. Rev. 89 (1989) 1861.
[2] A.P. Alivisatos, J. Phys. Chem. 100 (1996) 13226.
[3] M. Han, X. Gao, J.Z. Su, S. Nie, Nat. Biotechnol. 19 (2001) 631.
[4] J.K. Jaiswal, H. Mattoussi, J.M. Mauro, S.M. Simon, Nat. Biotechnol. 21 (2003) 47.
[5] A.M. Smith, X. Gao, S. Nie, Photochem. Photobiol. 80 (2004) 377.
[6] I.L. Medintz, H.T. Uyeda, E.R. Goldman, H. Mattoussi, Nat. Mater. 4 (2005) 435.
[7] E.R. Goldman, A.R. Clapp, G.P. Anderson, H.T. Uyeda, J.M. Mauro, I.L. Medintz, H. Mattoussi, Anal. Chem. 76 (2004) 684.
[8] E.R. Goldman et al., J. Am. Chem. Soc. 127 (2005) 6744.
[9] C.Y. Zhang, H.C. Yeh, M.T. Kuroki, T.H. Wang, Nat. Mater. 4 (2005) 826.
[10] I.L. Medintz, A.R. Clapp, H. Mattoussi, E.R. Goldman, B. Fisher, J.M. Mauro, Nat. Mater. 2 (2003) 630.
[11] C.A. Mirkin, R.L. Letsinger, R.C. Mucic, J.J. Storhoff, Nature 382 (1996) 607.
[12] W.C.W. Chan, S. Nie, Science 281 (1998) 2016.
[13] K. Hanaki, A. Momo, T. Oku, A. Komoto, S. Maenosono, Y. Yamaguchi, K. Yamamoto, Biochem. Biophys. Res. Commun. 302 (2003) 496.
[14] R. Mahtab, H.H. Harden, C.J. Murphy, J. Am. Chem. Soc. 122 (2000) 14.
[15] G.P. Mitchell, C.A. Mirkin, R.L. Letsinger, J. Am. Chem. Soc. 121 (1999) 8122.
[16] X. Wu et al., Nat. Biotechnol. 21 (2003) 41.
[17] H. Mattoussi, J.M. Mauro, E.R. Goldman, G.P. Anderson, V.C. Sundar, F.V. Mikulec, M.G. Bawendi, J. Am. Chem. Soc. 122 (2000) 12142.
[18] H. Mattoussi, J.M. Mauro, E.R. Goldman, G.P. Anderson, V.C. Sundar, F.V. Mikulec, M.G. Bawendi, Phys. Status Solidi (B) 224 (2001) 277.
[19] W.R. Algar, U.J. Krull, Langmuir 22 (2006) 11346.
[20] E. Chang, J.S. Miller, J. Sun, W.W. Yu, V.L. Colvin, R. Drezek, J.L. West, Biochem. Biophys. Res. Commun. 334 (2005) 1317.
[21] D. Zhou, J.D. Piper, C. Abell, D. Klenerman, D.-J. Kang, L. Ying, Chem. Commun. (2005) 4807.

[22] R. Gill, I. Willner, I. Shweky, U. Banin, J. Phys. Chem. B 109 (2005) 23715.
[23] R. Elghanian, J.J. Storhoff, R.C. Mucic, R.L. Letsinger, C.A. Mirkin, Science 277 (1997) 1078.
[24] B.M. Lingerfelt, H. Mattoussi, E.R. Goldman, J.M. Mauro, G.P. Anderson, Anal. Chem. 75 (2003) 4043.
[25] M. Dahan, S. Lévi, C. Luccardini, P. Rostaing, B. Riveau, A. Triller, Science 302 (2003) 442.
[26] F. Chen, D. Gerion, Nano Lett. 4 (2004) 1827.
[27] S. Wang, N. Mamedova, N.A. Kotov, W. Chen, J. Studer, Nano Lett. 2 (2002) 817.
[28] Q. Wang et al., J. Am. Chem. Soc. 129 (2007) 6380.
[29] V.R. Hering, G. Gibson, R.I. Schumacher, A. Faljoni-Alario, M.J. Politi, Bioconjugate Chem. 18 (2007) 1705.
[30] D. Neuman, A.D. Ostrowski, A.A. Mikhailovsky, R.O. Absalonson, G.F. Strouse, P.C. Ford, J. Am. Chem. Soc. 130 (2008) 168.
[31] Y. Matsumoto, R. Kanemoto, T. Itoh, S. Nakanishi, M. Ishikawa, V. Biju, J. Phys. Chem. C 112 (2008) 1345.
[32] W.R. Algar, U.J. Krull, Anal. Chim. Acta 581 (2007) 193.
[33] B.-K. Pong, B.L. Trout, J.-Y. Lee, Langmuir 24 (2008) 5270.
[34] J.R. Lakowicz, Principles of Fluorescence Spectroscopy, Kluwer Academic/Plenum, New York, 1999.
[35] M.G. Bawendi, P.J. Carroll, W.L. Wilson, L.E. Brus, J. Chem. Phys. 96 (1992) 946.
[36] V.I. Klimov, D.W. McBranch, Phys. Rev. Lett. 80 (1998) 4028.
[37] D.F. Underwood, T. Kippeny, S.J. Rosenthal, J. Phys. Chem. B 105 (2001) 436.
[38] M.D. Garrett, M.J. Bowers II, J.R. McBride, R.L. Orndorff, S.J. Pennycook, S.J. Rosenthal, J. Phys. Chem. C 112 (2008) 436.
[39] V.I. Klimov, J. Phys. Chem. B 104 (2000) 6112.
[40] S. Jeong, M. Achermann, J. Nanda, S. Ivanov, V.I. Klimov, J.A. Hollingsworth, J. Am. Chem. Soc. 127 (2005) 10126.
[41] T. Inokuma, T. Arai, M. Ishikawa, Phys. Rev. B 42 (1990) 11093.
[42] R. Simha, H.L. Frisch, F.R. Eirich, J. Phys. Chem. 57 (1953) 584.
[43] C.J. Murphy, G.C. Lisensky, L.K. Leung, G.R. Kowach, A.B. Ellis, J. Am. Chem. Soc. 112 (1990) 8344.
[44] R. Mahtab, J.P. Rogers, C.J. Murphy, J. Am. Chem. Soc. 117 (1995) 9099.
[45] C.A. Sprecher, W.C. Johnson Jr., Biopolymers 21 (1982) 321.
[46] R. Sarkar, S.K. Pal, Biopolymers 83 (2006) 675.
[47] R. Jin, G. Wu, Z. Li, C.A. Mirkin, G.C. Schatz, J. Am. Chem. Soc. 125 (2003) 1643.
[48] S.D. Goodman, H.A. Nash, Nature 341 (1989) 251.
[49] A.H. Elcock, J.A. McCammon, J. Am. Chem. Soc. 118 (1996) 3787.